

# Polarized OLED on a flexible optical anisotropic substrate for mobile display

**Byoungchoo Park\*, Chan Hyuk Park, Mina Kim, and Mi-young Han**

Dept. of Electrophysics, Kwangwoon Univ., Seoul 139-701, Korea

Tel.:82-2-940-5237, E-mail: bcpark@kw.ac.kr

**Keywords:** OLED, flexible, polarization, photonic anisotropic substrate

## Abstract

*We present highly polarized light emissions from an OLED on a flexible photonic anisotropic substrate. It was found that the polarization direction of emitted electroluminescent light corresponded to the ordinary-axis of the photonic anisotropic substrate. Furthermore, it was also found that luminous polarized electroluminescence over  $4,500 \text{ cd/m}^2$  was produced with high peak efficiency of  $6 \text{ cd/A}$  and high polarization ratio over 25.*

## 1. Introduction

Since the early pioneering work on efficient organic light-emitting devices (OLEDs) based on both small molecules and polymers, OLEDs have attracted a great deal of research interest due to their promising applications in full-color flat-panel mobile displays [1-5]. Almost all previous work carried out on organic electroluminescent (EL) light emission has involved unpolarized EL light emission. However, a number of studies have demonstrated linearly polarized EL emissions [6-9]. Such work was done because polarized EL emission from OLEDs is potentially useful in a number of applications, especially for mobile display. In order to design and manufacture such applications, a high degree of polarization ratio (*PR*) of emitting light is needed. In most cases, linearly polarized EL emissions were demonstrated for uniaxially orientated materials of liquid crystalline polymers or oligomers incorporated in emissive layers: the methods that are commonly used for the uniaxial alignment of such layers include the Langmuir-Blodgett technique [6], rubbing/shearing of the film surface [7, 8], mechanical stretching of the film [9, 10], orientation on pre-aligned substrates [11,

12], precursor conversion on aligned substrates [13], epitaxial vapour deposition [14], and the friction-transfer process approach [15, 16]. Although there have been a number of such efforts to achieve linearly polarized EL emission, the polarization ratio and the device performance (in terms of brightness and efficiency) of the devices reported are still insufficient for most applications. We herein propose an approach different from the conventional methods, which make use of uniaxially oriented materials. This has enabled us to achieve a high degree of linear polarization with high brightness and efficiency by using a flexible photonic anisotropic substrate, instead of an optically isotropic substrate such as glass. In this report, we describe the polarization of light emission from OLEDs that use a flexible photonic multilayer substrate [17], instead of the conventional glass substrate. By using such a substrate, we demonstrate the potential for highly polarized light emission from OLEDs.

## 2. Experimental

The sample OLEDs were prepared by placing an organic EL layer between an anode and a cathode on a flexible transparent photonic film in the following sequence: a flexible transparent photonic film substrate//a transparent anode//a hole-injecting buffer layer//an EL layer//an electron-injecting layer//a cathode. For the flexible transparent photonic film, a commercial multilayer reflecting polymer polarizer film (3M) was used. The film was approximately  $\sim 90 \mu\text{m}$  thick and the wavelength of the reflection band was in an approximate range of  $400 \sim 800 \text{ nm}$ . After routine cleaning of the flexible transparent photonic film using ultraviolet-ozone treatment, a flexible

semi-transparent thin Au layer was deposited (90 nm, 40 ohm/square) by sputtering it on the flexible transparent photonic film to form the anode. This Au anode was used in preference to the typical rigid indium-tin-oxide (ITO) anode in order to preserve the flexibility of the transparent photonic substrate. The optical transmittance of the Au electrode was about 60 % in the visible wavelength region. A solution of PEDOT:PSS (poly(3,4-ethylenedioxythiophene):poly(4-styrenesulphonate), Bayer) was spin-coated on the Au anode in order to produce the hole-injecting buffer layer. Subsequently, in order to form an EL layer, S-OLED ink (Green) was also spin-coated on the PEDOT:PSS layer. The emission peak wavelength of S-OLED ink was ~510 nm with a full width at half maximum (FWHM) of ~85 nm. The thicknesses of the PEDOT:PSS and EL layers were adjusted to be about 40 nm and 80 nm, respectively. In order to form the electron-injecting layer, a ~1 nm thick  $\text{Cs}_2\text{CO}_3$  interfacial layer was formed on the EL layer using thermal deposition (0.02 nm/s) at a base pressure less than  $2 \times 10^{-6}$  Torr with a shadow-mask that had  $3 \times 3$  mm<sup>2</sup> square apertures. Finally, a pure Al (~50 nm thick) cathode layer was formed on the interfacial layer using thermal deposition under the same vacuum condition. For comparison, we also fabricated reference devices using a glass substrate in place of the flexible transparent photonic substrate.

### 3. Results and discussion

Figure 1(a) shows a photograph of the flexible photonic multilayer substrate used. As shown in the photograph, the substrate is easy to bend and quite transparent. Figure 1(b) shows a scanning electron microscopy (SEM) image of the cross-sectional structure of the flexible photonic multilayer substrate. The SEM image shows clearly that the uniform layers of the two alternating layered elements of [a/b] are formed of multiple stacks with different refractive indices. The optical anisotropy of the flexible photonic multilayer substrate may be seen by inspecting the polarized microphotograph of the substrate between crossed polarizers at four angles of sample rotation of the film substrate, as shown in Fig. 2(a). This figure shows that the film substrate has a clear optical birefringence. We were able to define the orientation of the two optical axes,  $x$  and  $y$ , for the photonic film substrate from the darkest views of the polarized microphotographs. The polarized transmittance spectra from the photonic film substrate were then observed for the two incident lights

polarized linearly along the  $x$  and  $y$  axes, as shown in Fig. 2(b). From this figure, it is clear that the nature of the reflection bands depends strongly on the polarization of the incident light, and the polarized transmission spectra are thus quite different from each other. When measured in the  $y$  direction, the transmission spectrum shows a strong and broad reflection band, while in the  $x$  direction, there is no reflection band in the wide visible wavelength range that incorporates red, green, and blue light. It is thus evident that the birefringence causes the reflecting band structure to be polarized and that the  $x$  and  $y$  axes represent the ordinary ( $o$ ) and extraordinary ( $e$ ) axes, respectively. Note that the  $o$  axis is consistent with the passing axis and the  $e$  axis represents the blocking axis of the photonic film substrate. The average extinction ratio of the film substrate used was estimated to be about 16:1 in the wavelength region between 470 and 700 nm.

Next, in order to study the EL characteristics of the sample OLEDs, we observed the current density-luminance-voltage ( $J$ - $L$ - $V$ ) characteristics, as shown in Fig. 3(a). It is clear from this figure that both the charge-injection and turn-on voltages are below 4.0 V, with sharp increases in the  $J$ - $L$ - $V$  curves. The EL brightness reaches ~4,500 cd/m<sup>2</sup> at 14.5 V. This performance of the sample OLED with respect to luminescence is nearly the same as that of the

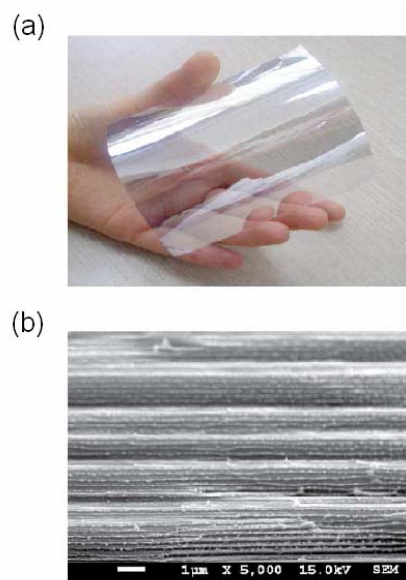


**Fig. 1. (a) Photograph showing the flexible transparent photonic film. (b) SEM image of the cross-section of the photonic film.**

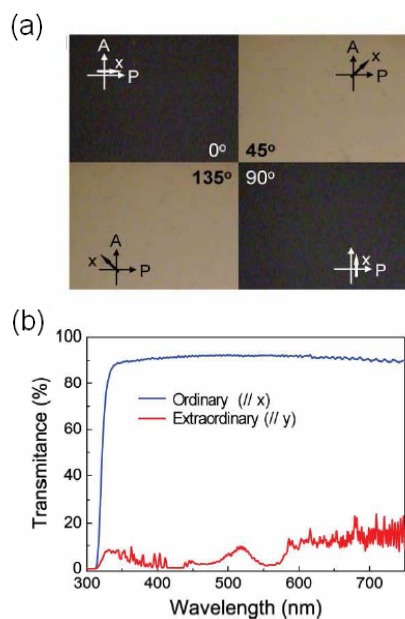


**Fig. 2. (a) Polarized microphotographs under crossed polarizers. (b) Polarized transmittance spectra for incident light polarized linearly along the  $x$  (ordinary) and  $y$  (extraordinary) axes.**

reference device using a conventional linear dichroic polarizer film, which showed ca.  $5,000 \text{ cd/m}^2$  at 14.5 V. In contrast, as shown in Fig. 3(b), the peak efficiencies of the sample OLED are much higher than those of the reference device. In order to understand the observed EL characteristics of the sample device, we also measured the polarization characteristics, as shown in Fig. 3(c). Figure 3(c) shows the polarized EL emission spectra for the polarizations along the  $o$  (blue solid curves) and  $e$  (red solid curves) axes at normal incidence ( $0^\circ$ ). The curves represented by the dotted lines show the total spectra ( $o + e$ ). It may be seen that the broad emission spectra are quite similar to that of the reference device, which coincided with the EL emission spectra of conventional OLED devices that have been reported elsewhere. This figure also shows that polarized EL emission spectra depend strongly on the polarization state, and that the sample OLED exhibits highly polarized EL emission over the entire range of emission spectra. For the sample device used, the  $PR$  ( $PR = I_o / I_e$ ) for the integrated EL intensities of the parallel and perpendicularly polarized EL emission was approximately 25. This ratio is significantly higher than that of the reference devices, which showed a  $PR$  of 1 (unpolarized light emission).

Next, as shown in Fig. 4, we observed the operating polarized OLED sample ( $3 \times 3 \text{ mm}^2$ , 10 V) for the

polarizations along the  $o$  and  $e$  axes of the photonic film substrate. It may be seen from the figure that under a rotatable linear dichroic polarizer, the fabricated sample OLED is fairly luminous and highly polarized along the ordinary axis of the photonic film substrate. From the above results, we conclude that a flexible polarized OLED with a high polarization ratio was fabricated successfully using the photonic film substrate.

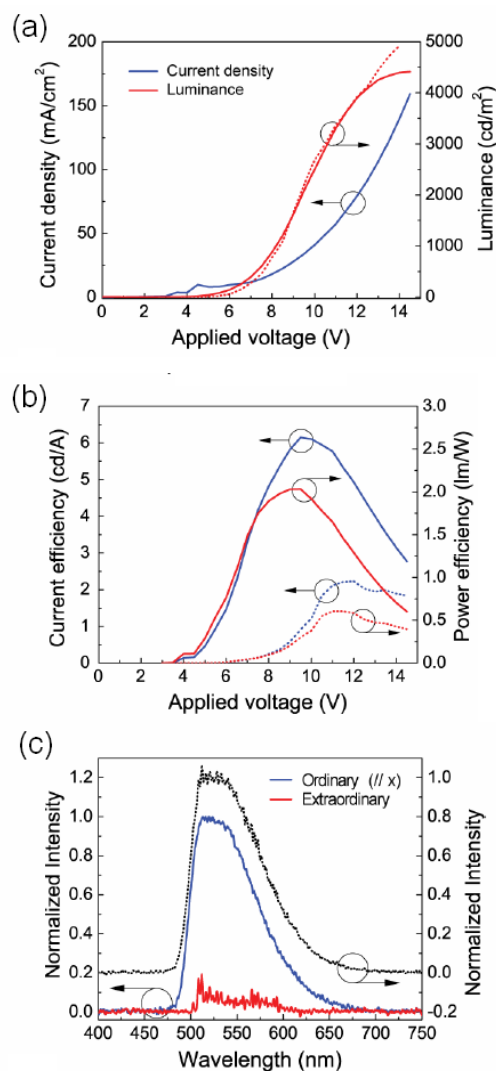


**Fig. 3. (a)  $J$ - $V$  and  $L$ - $V$  and (b) current efficiency-voltage and power efficiency-voltage of the sample device. The dotted curves show the characteristics of the reference device. (c) Polarized EL emission spectra along the  $o$  (red solid curves) and  $e$  (blue solid curves) axes of the polarized OLED.**

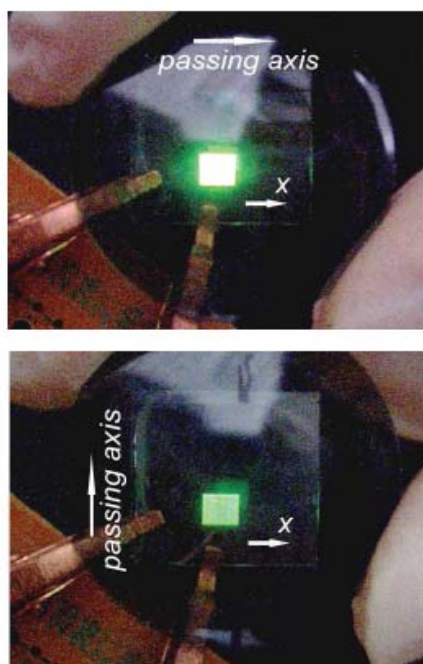


**Fig. 4. Photographs showing the operating polarized OLED sample ( $3 \times 3 \text{ mm}^2$ , 10 V) for the polarizations along the  $o$  (upper) and  $e$  (lower) axes of the flexible photonic substrate under a rotating linear dichroic polarizer.**

#### 4. Summary

In this study, we fabricated a flexible, polarized, and luminous OLED using a flexible photonic substrate for mobile display. It is shown that EL brightness over  $4,500 \text{ cd/m}^2$  were produced using the sample OLED with high peak efficiencies in excess of  $6 \text{ cd/A}$  and  $2 \text{ lm/W}$ . Furthermore, it was also shown that a high polarization ratio of up to 25 was possible over the whole emission brightness range. These results show that using the flexible photonic substrate enables the development of flexible OLEDs with highly polarized luminescence emissions. By combining the device reported here with luminous EL layers reported elsewhere, it will be possible to develop highly efficient polarized OLEDs that have a wide range of optical applications of mobile display.

#### Acknowledgement

The authors would like to acknowledge the financial support from Korea Science and Engineering Foundation (KOSEF, Project No. 2009-0077378).

#### 5. References

1. C. W. Tang and S. A. Van Slyke, *Appl. Phys. Lett.*, **51**, pp913-915 (1987)
2. R. H. Friend, R. W. Gymer, A. B. Holmes, J. H. Burroughes, R. N. Marks, C. Taliani, D. D. C. Bradley, D. A. Dos Santos, J. L. Bredas, M. Logdlund, and W. R. Salaneck, *Nature (London)*, **397**, pp121-128 (1999).
3. M. A. Baldo, S. Lamansky, P. E. Burrows, M. E. Thompson, and S. R. Forrest, *Appl. Phys. Lett.*, **75**, pp4-6 (1999)
4. M. Ikai, S. Tokito, Y. Sakamoto, T. Suzuki, and Y. Taga, *Appl. Phys. Lett.*, **79**, pp156-158 (2001).
5. C. Adachi, M. E. Thompson, and S. R. Forrest, *IEEE J. Sel. Top. Quantum Electron.*, **8**, pp372-377 (2002).
6. V. Cimrova, M. Remmers, D. Neher, and G. Wegner, *Adv. Mater.*, **8**, pp146-149 (1996).
7. M. Jandke, P. Strohmriegl, J. Gmeiner, W. Brutting, and M. Schwoerer, *Adv. Mater.*, **11**, pp1518-1521 (1999).
8. D. X. Zhu, H. Y. Zhen, H. Ye, and X. Liu, *Appl. Phys. Lett.*, **93**, pp163309 (2008).
9. P. Dyreklev, M. Berggren, O. Inganäs, M. R. Andersson, O. Wennerstrom, T. Hjertberg, *Adv. Mater.*, **7**, pp43-45 (1995).
10. C. C. Wu, P. Y. Tsay, H. Y. Cheng, and S. J. Bai, *J. Appl. Phys.*, **95**, pp 417-423 (2004).
11. M. Grell and D. D. C. Bradley, *Adv. Mater.*, **11**, pp895-905 (1999).
12. K. Sakamoto, K. Miki, M. Misaki, K. Sakaguchi, M. Chikamatsu, and R. Azumi, *Appl. Phys. Lett.*, **91**, pp183509 (2007).
13. K. Pichler, R. H. Friend, P. L. Burn, and A. B. Holmes, *Synth. Met.*, **55**, pp454-459 (1993).
14. M. Era, T. Tsutsui and S. Saito, *Appl. Phys. Lett.*, **67**, pp2436-2438 (1995).
15. M. Misaki, Y. Ueda, S. Nagamatsu, M. Chikamatsu, Y. Yoshida, N. Tanigaki, and K. Yase, *Appl. Phys. Lett.*, **87**, pp243503 (2005).
16. M. Misaki, M. Chikamatsu, Y. Yoshida, R. Azumi, N. Tanigaki, K. Yase, S. Nagamatsu, and Y. Ueda, *Appl. Phys. Lett.*, **93**, pp023304 (2008).
17. M. F. Weber, C. A. Stover, L. R. Gilbert, T. J. Nevitt, and A. J. Ouderkerk, *Science*, **287**, pp2451-2456 (2000), and references therein.